

Impurity Free Vacancy Disordering (IFVD) of $\text{In}_x\text{Ga}_{1-x}\text{As}/\text{InP}$ Quantum Well Structures for Monolithic Integration of Different Optoelectronic Devices

P. L. Gareso

Department of Physics, Faculty of Mathematics and Natural Sciences, Hassanuddin University

ABSTRACT

Impurity free vacancy disordering (IFVD) technique has been used to study the atomic intermixing of $\text{In}_x\text{Ga}_{1-x}\text{As}/\text{InP}$ quantum well structures using a SiO_2 and a TiO_2 dielectric layer. Three different indium composition in InGaAs QWs were investigated, lattice-matched (LM), compressively-strained (CS) and tensile-strained (TS). Based on Photoluminescence results, the atomic intermixing between the quantum well and the barrier regions enhanced when the samples were coated with SiO_2 layers. Although TiO_2 layers were able to suppress the intermixing in InGaAs/InP system, the suppression was not significant compared to the $\text{AlGaAs}/\text{GaAs}$ system. Based on a fitting procedure that was deconvoluted from the photoluminescence spectra including theoretical modeling, the electron-heavy hole and electron-light hole transitions were identified and a ratio of the group V to the group III diffusion coefficients (k) were obtained. The k ratio of the InGaAs/InP samples capped with SiO_2 is relatively larger than of samples capped with TiO_2 layers.

Keywords: Atomic intermixing, IFVD, InGaAs/InP QWs

INTRODUCTION

Quantum well intermixing is a postgrowth method that enables the monolithic integration of different optoelectronic devices. This technique is used to modify the band gap in selected area of quantum well structures (QWs) through the intermixing of atoms in the quantum well and barrier regions (Li 2000; Marsh 1993). Intermixing in the active region can be achieved by several techniques including ion implantation (Li 2000; Marsh 1993; Paquette *et al.* 1997), impurity induced disordering (Deppe & Holonyak 1988), and impurity free vacancy disordering (Si *et al.* 1998; Cao *et al.* 1997). Among these various methods, IFVD has shown to be very effective for device application since it is simple and the amount of residual defects that are created by the intermixing process is much lower than by ion implantation and impurity diffusion. The IFVD technique has been discussed in the previous studies using $\text{InGaAs}/\text{AlGaAs}$ (Cao *et al.* 1997) and $\text{InGaAs}/\text{AlGaAs}$ QW structures. However, this is very different from the InGaAs/InP system that will be discussed in this study.

In this study, $\text{In}_x\text{Ga}_{1-x}\text{As}/\text{InP}$ quantum well structures were used due to their suitability for 1.3 and 1.5 μm wavelength optical fibre communication applications (Temkin *et al.* 1990). This system has been used for application in different varieties of optoelectronic devices such as modulators

(Koren *et al.* 1987), waveguides (Koren *et al.* 1987) and laser (Temkin *et al.* 1990). However, intermixing of the InGaAs/InP system is more complicated than in the $\text{AlGaAs}/\text{GaAs}$ QWs, or strained $\text{InGaAs}/\text{GaAs}$ QWs.

In the latter two structures, only group III interdiffusion occurs (In and Ga) since the concentration of As across the barrier/well interface remains constant. InGaAs/InP system, on the other hand, both group V (As,P) and group III (In,Ga) atoms could drive the well/barrier interdiffusion and they contribute differently to the interdiffusion between the quantum well and the barrier regions. Previous studies on the interdiffusion in this system using ion implantation and IFVD have reported varying ratios between group V and group III diffusion coefficients (Chen *et al.* 1999; Si *et al.* 1998; Ryu *et al.* 1997).

Interdiffusion in this system has an added degree of complexity, since there is the possibility of both group III and group V interdiffusion across the InP/InGaAs interface, unlike the $\text{InGaAs}/\text{AlGaAs}$ quantum well system where only group III interdiffusion needs to be taken into account. Previous studies of InGaAs/InP interdiffusion using a range of techniques such as ion implantation induced intermixing and IFVD have reported varying ratio between group III and group V diffusion rates. As a result of the differences between the group III and the group V diffusion coefficients, a lattice-matched InGaAs/InP QW structure for example will no longer remain to

be lattice matched after interdiffusion and thus strain will be introduced into the system.

METHODS

Three different indium composition of InGaAs QWs, lattice-matched (LM), compressively-strained (CS) and tensile-strained (TS) were grown on (100) semi-insulating InP substrates by low pressure metalorganic chemical vapor deposition (MOCVD) with a growth temperature of 650°C. Each structure consists of a 600 nm InP buffer layer, a 5 nm $\text{In}_x\text{Ga}_{1-x}\text{As}$ QW, a 200 nm InP layer followed by a 100 nm $\text{In}_{0.53}\text{Ga}_{0.47}\text{As}$ capping layer. Single dielectric layers of either SiO_2 or TiO_2 were deposited on the top layer of the samples (Figure 1). Silicon dioxide with a thickness of 200 nm thick was deposited by plasma enhanced chemical vapor deposition (PECVD) using a $\text{N}_2\text{O}/\text{SiH}_4$ mixture at room temperature. Each of the SiO_2 layer were half etched off by 10% HF after deposition to provide a reference region. TiO_2 layers with a nominally thickness of 200 nm were deposited by electron beam evaporation. In order to create the reference regions, half of each sample was covered with a mask prior to the TiO_2 deposition. All the samples were annealed under Ar flow in a rapid thermal annealer in the temperature range of 700-850°C for 60 sec.

During the annealing process the samples were sandwiched between an InP proximity layer that covered the substrate and a GaAs proximity layer next that covered the InGaAs capping layers. Room temperature photoluminescence (PL) measurements were performed to characterize the energy shift of the emission from the active region, using a diode-pumped solid-state frequency doubled green laser at 532 nm for excitation and a cooled InGaAs photodetector at the output slit of a 0.5 m monochromator. After annealing, the InGaAs capping layers were removed to improve the

intensity of the PL spectra. The relative PL emission energy shift between the dielectric coated side and the reference (uncoated side) region was calculated.

RESULTS AND DISCUSSION

Comparison between samples with top InP and InGaAs layers

There is a very significant difference in the degree of SiO_2 induced intermixing when the samples have either a top InP or InGaAs layer as shown in Figure 2. When the SiO_2 layer was deposited directly on InGaAs, large energy shifts were observed in all the three samples, especially at 800°C, when the diffusion of Ga vacancies became appreciable. In contrast when SiO_2 was deposited directly on InP, hardly any significant energy shifts were observed in all three samples. Indeed, at 800°C, a small redshift was observed for the CS and TS QW.

In the case of $\text{SiO}_2/\text{InGaAs}$, group III vacancies were generated at the interface as a result of outdiffusion of Ga atoms from the InGaAs layer to the SiO_2 . Due to the larger thermal expansion coefficient of InGaAs in comparison to SiO_2 (Table 1), the InGaAs layer experienced a compressive strain which promoted the diffusion of the group III vacancies across the QW. Although it is expected that group III diffusion in InGaAs/InP QW will create a redshift, this is not observed from the experimental results.

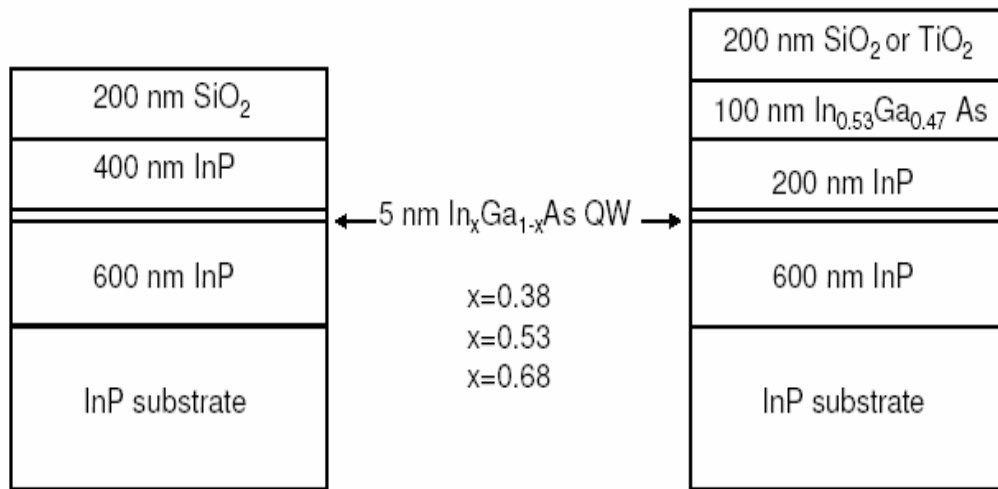


Figure 1. The schematic diagram of samples used in the IFVD study.

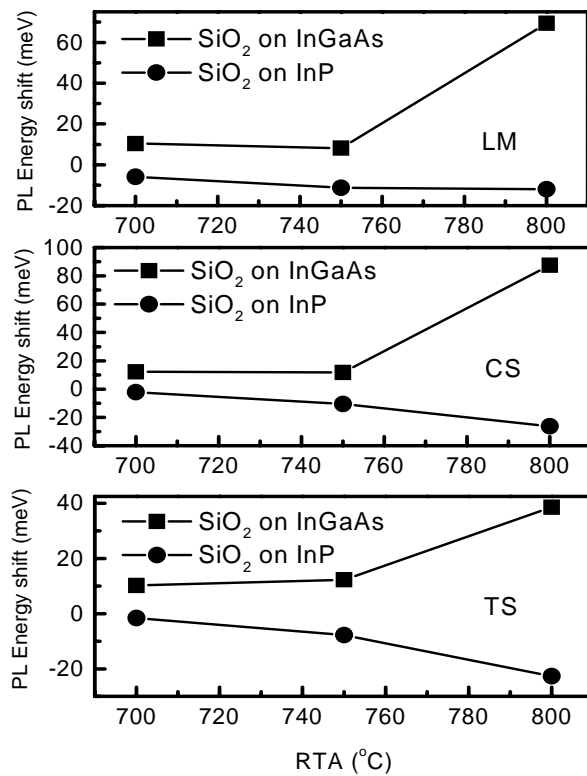


Figure 2. The PL energy shift of lattice-matched (LM), compressively-strained (CS), and tensile-strained (TS) $\text{In}_x\text{Ga}_{1-x}\text{As}/\text{InP}$ QWs capped with SiO_2 layers as a function of annealing temperature.

Table 1. Thermal expansion coefficients for InGaAs and InP and various dielectric layers.

Material	Thermal expansion coefficient ($10^{-6} \text{ }^{\circ}\text{C}^{-1}$)
SiO ₂	0.52
InGaAs	5.25
InP	6.86
TiO ₂	8.19

It was reported that initial group III interdiffusion will increase the In composition in the QW and consequently increases the lattice constant (or strain) of the InGaAs with respect to the InP barrier and in order to minimize this strain, diffusion of P into the QW is encouraged (or outdiffusion of As from the QW) so as to reduce the strain (Carmody 2003). However, this is only true for the LM and CS QWs. For the TS QW, group III diffusion would only make the QW less (tensile) strained. It has been reported that the presence of Ga vacancies at the InGaAs/SiO₂ interface also results in the formation of As antisites, $\text{As}_{\text{Ga}} (\text{V}_{\text{Ga}} + \text{As}_i \rightarrow \text{As}_{\text{Ga}})$ (Deenapanray *et al.* 2002). Hence, this effect may also promote the diffusion on the group V sublattice, resulting in P diffusion into the QW and hence the observed blueshift. Indeed, the modeling results presented in later section show that diffusion occurs in both the group III and V sublattices, with the latter being a more dominant effect.

For SiO₂/InP samples, it has been shown that the In atoms also outdiffused into the SiO₂ layer upon annealing (Carmody 2003). Although the thermal expansion coefficient of InP is of the same order as that of InGaAs (and larger in comparison to that of SiO₂), the compressive strain generated at the InP does not promote the diffusion of group III vacancies. However, the very small degree of redshift at 800°C in this set of samples suggested that there is diffusion of the group III species albeit very small. The red shift may be due to enhanced thermal interdiffusion in the region with no capping layers. It is well known that InP has low surface melting temperature leading to significant thermal interdiffusion.

Comparison between SiO₂ and TiO₂ on InGaAs

The normalized graphs of the photoluminescence spectra of the TS, LM and

CS InGaAs/InP QW structures that were capped with SiO₂ and TiO₂ dielectric layers taken before and after annealing were depicted in Figure.3. For the samples capped with SiO₂, a small energy shift was observed for LM, TS, and CS after annealing at 700°C and 750°C. Annealing the samples at 800°C resulted in a significant shift in comparison to the as-grown samples. In the case of TiO₂ capped samples, a small energy shift was observed after annealing them at either 700°C or 750°C compared to as-grown samples. A small enhancement in the wavelength shift was clearly observed when the samples were annealed at 800°C. The wavelength shift of the samples coating with TiO₂ layers is relatively smaller than the wavelength shift of SiO₂ capped samples at similar conditions. In addition to this, the PL linewidth of the TiO₂ capped samples is a bit narrow compare with the PL linewidth of SiO₂ cases. These results indicate that the TiO₂ capping layers are generally more effective than SiO₂ capping layers at suppressing the intermixing in In_xGa_{1-x}As/InP QWs.

A plot of the energy shift of LM,CS,TS samples as a function of annealing temperature with and without dielectric layers (SiO₂ and TiO₂) are shown in Figure 3. As can be seen in these figures, SiO₂ capped samples exhibit a large energy shift, and the amount of energy shift increases significantly with an increasing annealing temperature. Annealing at 850°C gives an energy shift of around 190 meV, 220 meV and 138 meV for LM, CS and TS samples, respectively. The large energy shift can be explained by strong intermixing caused by the generation of vacancies at the oxide/InGaAs interface. Most likely, in the SiO₂ case, during annealing the group III atoms outdiffuse from the InGaAs layers to the oxide layers, thus generating the group III vacancies. As a result of this, an excess of arsenic atoms form at the interface which then become an interstitial defect. Previous studies on the silica

treatment of GaAs samples reported that the formation of gallium vacancies (V_{Ga}) at the silica/GaAs interface which was under compressive stress will result in the formation of As interstitial, and as consequence As_{Ga} ($V_{Ga} + As_i \rightarrow As_{Ga}$) formation is also favoured (Deenapanray *et al.* 2002). This result shows that the formation of V_{Ga} might occur at the $SiO_2/InGaAs$ interface due to the solid solubility of gallium to the oxide layers. This can lead to an interdiffusion of the group V and the group III sublattices.

In addition to this, strain introduced at the $SiO_2/InGaAs$ interface is another possible explanation for the enhancement of the interdiffusion. Due to the larger thermal expansion coefficient of InGaAs ($\sim 5.3 \times 10^{-6} \text{ } ^\circ\text{C}^{-1}$) compare with SiO_2 ($\sim 0.52 \times 10^{-6} \text{ } ^\circ\text{C}^{-1}$), during annealing the InGaAs layers are under compressive strain causing the group III atoms to diffuse through into the quantum well regions. This initial group III interdiffusion will increase the indium composition in the quantum well region which consequently increases the lattice constant of the InGaAs with respect to the InP barrier, thus causing the quantum well to be under additional compressive strain. In order to minimize this strain, it is assumed that group V interdiffusion will also occur during annealing by increasing the P content of the quantum well and the As content of the barriers so that the lattice constant of the quantum well can be reduced (Carmody 2003).

The results of the CS structures confirmed this as shown in Figure 4 where the largest energy shift was observed after annealing at 850°C compare with LM and TS structures. Most likely in the CS structures, as the quantum well experience on additional compressive stress due to an increase of the indium content of the quantum well region, the quantum well in the CS structure becomes more compressively strained than in the LM and TS structures. In contrast to TS structures, although the initial group III interdiffusion causes the quantum well to shift toward compressive strain, the energy shift is relatively less compare to the CS and LM cases.

In the case of TiO_2 , a suppression of interdiffusion was observed after annealing

within a temperature range of 700°C to 800°C . The energy shift is smaller than in uncapped samples. However, a little improvement in the energy shift was shown after annealing at 850°C in the LM and CS samples but not in TS case. Due to the large thermal expansion of TiO_2 ($8.2 \times 10^{-6} \text{ } ^\circ\text{C}^{-1}$) in comparison to InGaAs ($5.3 \times 10^{-6} \text{ } ^\circ\text{C}^{-1}$), during RTA, near the $TiO_2/InGaAs$ interface region, TiO_2 becomes compressive and InGaAs tensile. These might cause a trapping of the group III vacancies in the region under stress which leads to the reduction of group III vacancies outdiffusing from InGaAs and thus the degree of intermixing. This explanation is confirmed for the samples annealed within the range of $700-800^\circ\text{C}$. In this regime, the TiO_2 effectively suppresses the intermixing. The suppression of interdiffusion in this system, however, is not significant compare with the AlGaAs/GaAs system. This is because in the latter system, only group III vacancies contribute the interdiffusion. At the same time, different degrees of intermixing were shown after annealing the samples at 850°C in which the enhancement of the interdiffusion was obviously seen. Most likely at this condition, a high temperature annealing might reduce the effect of strain at the $TiO_2/InGaAs$ interface, and thus reducing the gallium vacancies being trapped in the region under stress. Based on the results above, SiO_2 and TiO_2 are clearly seen affecting the degree of intermixing in $In_xGa_{1-x}As/InP$ QWs in fundamentally different ways. The group V sublattice is more preferable to promote intermixing when the samples are covered with SiO_2 layers. On the other hand, the group III sublattice dominates the intermixing process when the samples are capped with TiO_2 layers. Our results here are further confirmed in previous studies. Such work indicated that group III interdiffusion in InGaAs/InP is associated with a red shift, while blue shift is associated with a dominant group V interdiffusion. To what extent the group V and group III interdiffusion contribute to the intermixing will be obtained by the ratio of the diffusion coefficients of group V and group III sublattices.

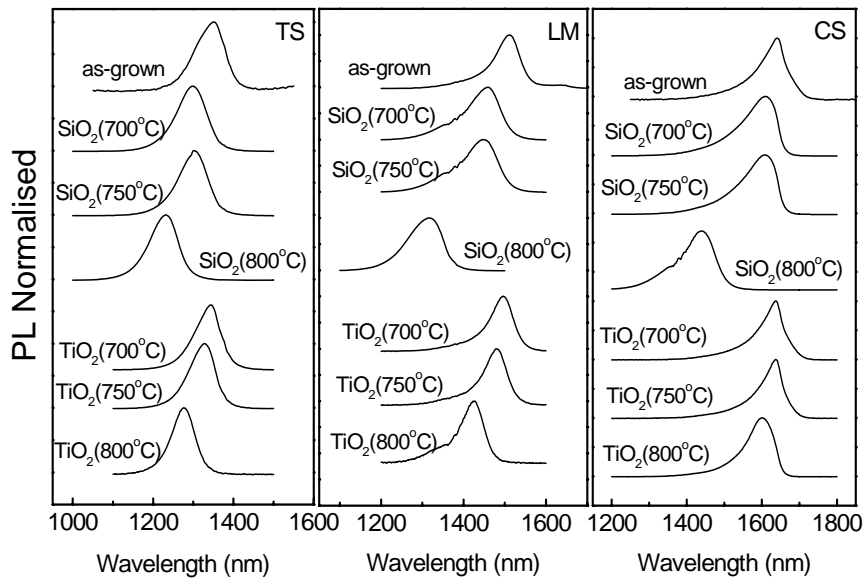


Figure 3. Room temperature photoluminescence (PL) spectra of tensile-strained (TS), lattice-matched (LM) and compressively-strained (CS) $\text{In}_x\text{Ga}_{1-x}\text{As}/\text{InP}$ QWs capping with SiO_2 and TiO_2 layers after annealing with various temperature from 700°C to 800°C . The PL spectra from as-grown samples are also shown as a comparison.

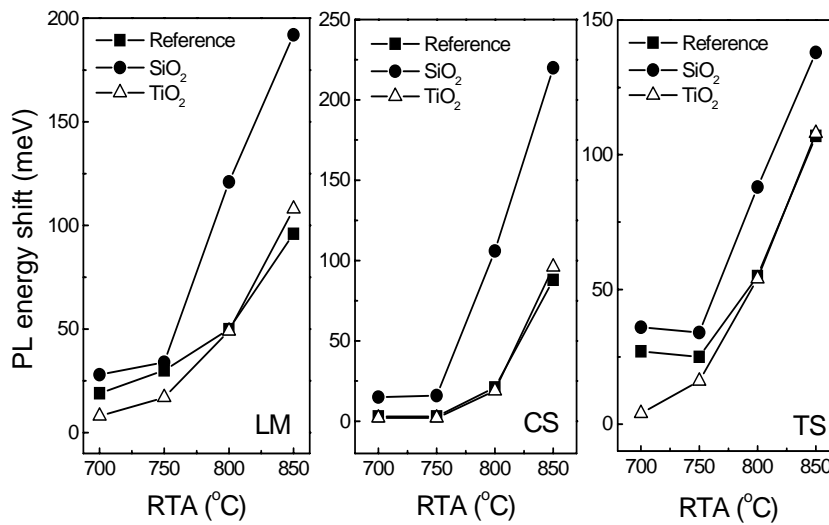


Figure 4. The PL energy shift of lattice-matched (LM), compressively-strained (CS), and tensile-strained (TS) $\text{In}_x\text{Ga}_{1-x}\text{As}/\text{InP}$ QWs with and without SiO_2 and TiO_2 layers as a function of annealing temperature.

In order to obtain the k ratio of group V and group III sublattices, the photoluminescence spectra was used to identify the electron-heavy hole and the electron-light hole transition energies. In addition to this, modeling of the conduction and valance band structure was

used to determine the ratio of the group V to group III diffusion coefficients. As can be seen from Fig.3, the luminescence spectra are not symmetric which indicates that the PL spectra consist of more than one peak overlapping peak. One component peak on the lower energy

side is related to the heavy-hole transitions and the other peak corresponds to the light-hole transitions. To extract these two component peaks, the peaks were deconvoluted using fitting procedures. After fitting (Fig.5), for the LM case capped with SiO₂, the electron-heavy-hole (C-HH) transitions for samples annealed at 750°C were observed at 0.856 eV and the electron-light-hole (C-LH) transitions were observed at 0.898 eV. In the case of TiO₂, the electron-heavy-hole (C-HH) transitions were observed at 0.839 eV and the electron-light-hole (C-LH) transitions were observed at 0.893 eV. These transitions allowed us to determine the magnitude of the diffusion length of group-V and group-III sublattices from which the ratio (*k*) of interdiffusion rates on the group-V and the group-III sublattices are determined. A similar approach has been used for TS and CS QWs to calculate the *k* ratio between diffusion coefficients of group-V and group-III sublattices.

It has been shown that the interdiffusion in III-V compound semiconductors is driven by vacancy diffusion (Carmody 2003). Interdiffusion occurs along concentration gradients causing the quantum well (QW) potential to become graded and causes a blueshift in the emission energy. The interdiffusion process can be modeled by Fick's law which is the general diffusion equation describing the time dependence of the concentration, *C*, as a function of a material parameter called the diffusivity, *D*, and the gradient of the concentration and is given below:

$$\frac{\partial c}{\partial t} = \nabla \circ (D \nabla c) \quad (1)$$

This equation can be solved in one dimension to give the concentration profile of a quantum well after diffusion.

$$C(z) = C_B + \frac{(C_w - C_B)}{2} \left\{ \operatorname{erf} \left(\frac{h-z}{L_D} \right) + \operatorname{erf} \left(\frac{h+z}{L_D} \right) \right\} \quad (2)$$

where *C_B* is the concentration of the barrier material and *C_w* is the concentration of the well. The amount of diffusion is characterised by the diffusion length, *L_D*, given by *L_D* = 2√*Dt*. For AlGaAs/GaAs and InGaAs/GaAs quantum wells, the group III vacancies provide the mechanism for interdiffusion since the group V atoms concentration (As) remain constant across the heterointerface. On the otherhand, for InGaAs/InP both group V and group III vacancies can contribute to the interdiffusion.

The theoretical modeling of the interdiffusion was carried out with an assumption that both group-V and group-III sublattices were Fickian for all the samples during the interdiffusion. Two independent coefficients *D_{III}* and *D_V*, characterizing the isotropic interdiffusion of group III and group V constituent elements were used, respectively. The factor *k* is defined as the ratio *L_V*/*L_{III}* are diffusion lengths corresponding to the two sublattices: *L_{III,V}* = 2√*D_{III,V}* *t*. The diffusion coefficients are assumed to be independent of the concentration of the diffusing element. The error function is used to simulate the interdiffusion at hetero-interfaces by creating a more parabolic-type profile instead of sharp step. From the composition profiles, the valence and conduction band profiles are calculated and the corresponding Schrödinger equations are solved using a transfer matrix method to provide the energies of the photoluminescence transitions. The layers are assumed to be fully strained and the material constants corresponding to each composition are taken from (Vurgaftman *et al.* 1991). The model does not include a calculation of the shift in the transition energy due to the excitonic binding energies or the quantum-confined Stark effects.

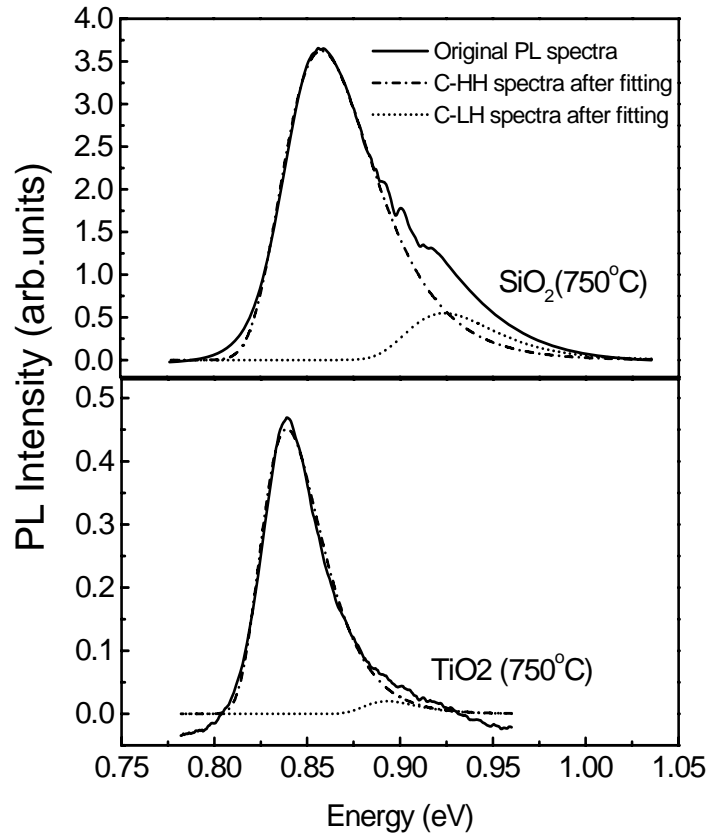


Figure 5. The photoluminescence spectra of InGaAs/InP lattice-matched after annealing at 750°C for 60 sec capping with SiO₂ and TiO₂ before and after fitting.

Based on the experimental and the modeling results, the k ratio of TS and LM and CS samples capped with SiO₂ was 1.15, 1.52 and 1.65, respectively. These values were higher than one indicating that the diffusion coefficients of group V sublattice was larger than that the diffusion coefficients of group III sublattice. In addition to this, for the TiO₂ case, the k ratio for TS, LM and CS was at 1.05, 1.06 and 1.15, respectively. These values were slightly higher than unity, indicating that the diffusion coefficient of group V is comparable to the diffusion coefficient of the group III sublattice.

CONCLUSION

In summary, we have investigated the influence of TiO₂ and SiO₂ layers on the atomic interdiffusion of group-V and group-III

sublattice in In_xGa_{1-x}As/InP quantum well structures using photoluminescence measurements at room temperature. Enhancement of the intermixing was observed for samples capped with SiO₂ layers. The largest energy shift was observed for CS SiO₂ capped structures after annealing at 850°C, while the interdiffusion was suppressed under TiO₂ layers. The degree of intermixing in both SiO₂ and TiO₂ capped samples is most likely due to the difference in the thermal expansion of the dielectric to the InGaAs layers. Based on the fitting results from photoluminescence spectra and theoretical modelling results, the interdiffusion rate of group V and group III sublattices (k) is higher for SiO₂ capped samples than in TiO₂ capped samples. This indicates that in SiO₂ layers, the group V is preferable promoting the interdiffusion between quantum well and barrier region.

While, group III sublattice is comparable with group V sublattice if the samples is capped with TiO₂ layers. In addition to this, the use of TiO₂ is a very attractive option for optoelectronic integration.

Acknowledgments

P.L.G acknowledges to H.H. Tan for providing the samples in this research and to Department of Higher Education of Indonesia (DIKTI) through DP2M for the financial support with contract number of 322/SP2H/DP2M/PP/III/2008.

REFERENCES

- Cao N, Elenkrig BB, Simmons JG & Thompson DA. 1997. *Appl. Phys. Lett.* **79**: 419.
- Carmody CY. 2003. *Defect Engineering of InP and InGaAs for optoelectronic Applications*, Ph.D. Thesis. The Australian National University,
- Charbonneau S, Poole PJ, Feng Y, Aers GC, Dion M, Davies M, Goldberg RD & Mitchell IV. 1995. *Appl. Phys. Lett.* **67**:2954.
- Chen H, Feenstra RM, Piva PG, Goldberg RD, Mitchell IV, Aers GC, Poole PJ & Charbonneau S. 1999. *Appl. Phys. Lett.* **75**(1): 79.
- Deenapanray PNK, Gong B, Lamb R, Martin A, Fu L, Tan HH & Jagadish C. 2002. *Appl. Phys. Lett.* **80**: 4351.
- Deppe DG & Holonyak NJr. 1988J. *Appl. Phys* **64**: R93.
- Koren U, Koch TL, Presting H & Miller BI. 1987. *Appl. Phys. Lett.* **50**: 368.
- Koren U, Miller BI, Koch TL, Boyd GD, Capik RJ & Soccolish CE. 1987. *Appl. Phys. Lett* **49**: 1602.
- Li EH. *Semiconductor Quantum Wells Intermixing* 2000. Gordon and Breach, Amsterdam.
- Marsh JH. 1993. *Semicond. Sci. Technol.* **8**: 1136.
- Micallef J. 2000. *Semiconductor Quantum Well Intermixing*, ed E. H. Lie. Amsterdam: Gordon and Breach.
- Paquette M, Beauvais J, Beerens J, Poole PJ, Charbonneau S, Miner CJ & Blaauw C. 1997. *Appl. Phys. Lett.* **71**: 3749.
- Ryu SW, Choe BD & Jeong WG. 1997. *Appl. Phys. Lett.* **71**(12): 167.
- Si SK, Yeo DH, Yoo KH & Kim SJ. 1998 IEEE. *J. Sel. Top. Quantum Electron* **4**:619.
- Si SK, Yeo DH, Yoon KH & Kim SJ. 1998. *J. Sel. Top. Quantum Electron* **4**:619.
- Tan HH, William JS, Jagadish C, Burke PT & Gal M. 1996. *Appl. Phys. Lett.* **68**: 2401.
- Temkin H, Tanbun T & Logan RA. 1990. *Appl. Phys. Lett.* **50**:1210.
- Temkin H, Tanbun EkT & Logan RA. 1990. *Appl. Phys. Lett* **56**: 1210.
- Vurgaftman I, Meyer JR & Ram-Mohan LR. 1991. *J. Appl. Phys* **89**:581.